

Miscibility of Block Copolymers and Surfactants in Lamellar Liquid Crystals

Kenji Aramaki,[†] Md. Khalid Hossain,[†] Carlos Rodriguez,[‡]
Md. Hemayet Uddin,[†] and Hironobu Kunieda^{*,†}

Graduate School of Environment and Information Sciences, Yokohama National University,
79-7 Tokiwadai, Hodogaya-ku, Yokohama 240-8501, Japan, and Universidad de Los Andes,
Escuela de Ingeniería Química, Merida 5101, Venezuela

Received July 23, 2003; Revised Manuscript Received September 20, 2003

ABSTRACT: The phase behavior and structures of liquid crystals in aqueous solution of Pluronic copolymers (P85; (PEO)₂₆(PPO)₄₀(PEO)₂₆, P105; (PEO)₃₇(PPO)₅₈(PEO)₃₇) mixed with nonionic surfactants (C₁₂EO₅, C_{18:1}EO₅) were investigated. In a binary water/P85 system, the sequence of self-assemblies is similar to that of the aqueous P105 system, and aqueous micellar solution, micellar cubic, hexagonal, and lamellar phases are successively formed. P85 forms a single lamellar liquid crystal (L_α) with C₁₂EO₅ in water at high concentration, whereas two L_α phases coexist in the water/P105/C₁₂EO₅ system. Two coexisting lamellar phases become identical at a critical point upon replacing P105 with P85. We calculated the average cross-sectional area, a_s , at the hydrophobic interface using SAXS data. The partial molecular areas of copolymer, a_s^P , and surfactant, a_s^S , were also evaluated from a_s values obtained at different compositions of the copolymer–surfactant mixture. It was found that a_s^P decreases and a_s^S slightly increases in the copolymer L_α phase with increasing the surfactant mixing fraction in the copolymer–surfactant mixture.

I. Introduction

Amphiphilic triblock copolymers consisting of a relatively hydrophobic poly(oxypropylene) (PPO) middle block and two hydrophilic poly(oxyethylene) (PEO) end blocks are commercially available in a large variety of molecular weights and PEO/PPO ratios and are referred as Poloxamers or Pluronic.¹ PEO–PPO–PEO triblock copolymer forms many varieties of self-assemblies in water or in water–oil depending on concentration, molecular weight, PEO/PPO block ratio, solvent type, etc.^{2–5}

There are many studies on ionic–ionic and ionic–nonionic surfactant–copolymer systems, but only a few on nonionic surfactant and nonionic amphiphilic copolymer mixed systems in a wide range of compositions, simply because they do not normally show significant interactions due to the absence of electric charges. Recently, an interesting phase behavior was reported in a surfactant–copolymer system with poly(oxyethylene) alkyl ether and poly(oxyethylene)–poly(dimethylsiloxane) diblock copolymer.⁶ In the phase diagram of this aqueous nonionic surfactant–nonionic copolymer system, two lamellar phases coexist in a certain range of copolymer/surfactant ratio, one containing surfactant-rich thin bilayers and the other copolymer-rich thick bilayers. Cell membranes have a structure similar to that of lamellar liquid crystals, with large molecules such as enzymes and proteins embedded in the bilayers.⁷ Hence, it is relevant to study the miscibility of large molecules in amphiphilic bilayers, and nonionic surfactant–copolymer systems can be used as models for this purpose.

In our previous paper,⁸ we reported that two lamellar phases also coexist in the water/P105/C₁₂EO₅ system.

It was again observed that surfactant molecules are incorporated in the copolymer-rich lamellar phase whereas the copolymer is barely incorporated in the surfactant bilayer. Such kinds of coexisting lamellar phases are observed only in a few systems.⁹ If the molecular size of the copolymer is reduced, it can be expected that copolymer and surfactant molecules would mix in the lamellar phases in the whole range of copolymer/surfactant mixing ratios. Then, the mixing behavior of two amphiphiles with a large difference in size would be clarified.

In this paper, we have chosen Pluronic P85 as a copolymer with a molecular weight lower than P105, but with the same weight ratio of hydrophilic chain to total copolymer, $f = 0.5$. First, we compare the phase behavior of P85 in water with that of P105. Then, the miscibility of these copolymers with penta(oxyethylene) dodecyl ether (C₁₂EO₅) in a lamellar liquid crystal is studied. Finally, the miscibility of these copolymers with penta(oxyethylene) oleyl ether (C_{18:1}EO₅) is compared with the results obtained for C₁₂EO₅ systems.

II. Experimental Section

A. Materials. The poly(oxyethylene) (PEO)–poly(oxypropylene) (PPO)–poly(oxyethylene) (PEO) triblock copolymers (PEO)₂₆(PPO)₄₀(PEO)₂₆ and (PEO)₃₇(PPO)₅₈(PEO)₃₇ with the trade name Pluronic P85 and Pluronic P105, respectively, are obtained as a gift from BASF Corp., Parsippany, NJ, and will be regarded as P85 and P105, respectively, from onward in the present paper. P85 has a nominal molecular weight of 4600 while P105 has a nominal molecular weight of 6500. Homogeneous penta(oxyethylene) dodecyl ether (C₁₂EO₅) was purchased from Nikko Chemicals Co., Japan, and penta(oxyethylene) oleyl ether (C_{18:1}EO₅) was kindly donated by NOF Co., Japan. The hydrophobic part (oleyl group) of C_{18:1}EO₅ is extremely pure, but there is a distribution of poly(oxyethylene) chain lengths.¹⁰ The molar volumes of amphiphiles and their hydrophilic parts are presented in Table 1. The density of P85 in the liquid state at 25 °C was measured using a digital density meter (Anton Paar, DMA-40), according to the procedure describe in a previous paper.⁸

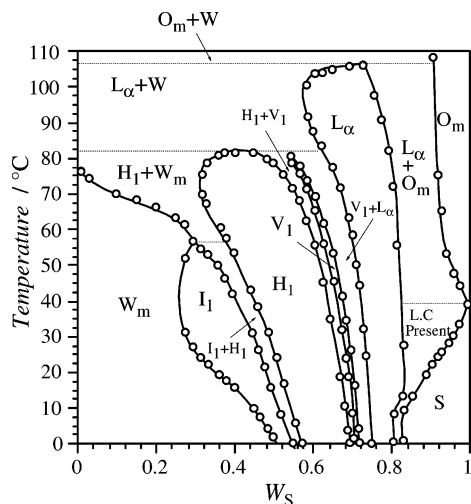
[†] Yokohama National University.

[‡] Universidad de Los Andes.

* Corresponding author: phone and Fax +81-45-339 4190; e-mail kunieda@ynu.ac.jp.

Table 1. Molar Volumes of Amphiphiles and Their Hydrophilic Parts

amphiphile	molar vol of amphiphile (cm ³ mol ⁻¹)	vol of hydrophilic EO chain (cm ³ mol ⁻¹)
P85	4307	2026
P105	6035 ^a	2880
C ₁₂ EO ₅	418 ^b	203 ^b
C _{18:1} EO ₅	516 ^c	203 ^c

^a From ref 8. ^b From ref 11. ^c From ref 10.**Figure 1.** Phase diagram of the binary water/P85 system as a function of the weight fraction of copolymer, W_s .

The volume fraction of the hydrophilic part in total amphiphile, f , is almost equal to 0.5 for all the amphiphiles except C_{18:1}EO₅, which is slightly lipophilic although it mainly forms a lamellar liquid crystal in water.

Millipore filtered water was used to prepare the samples.

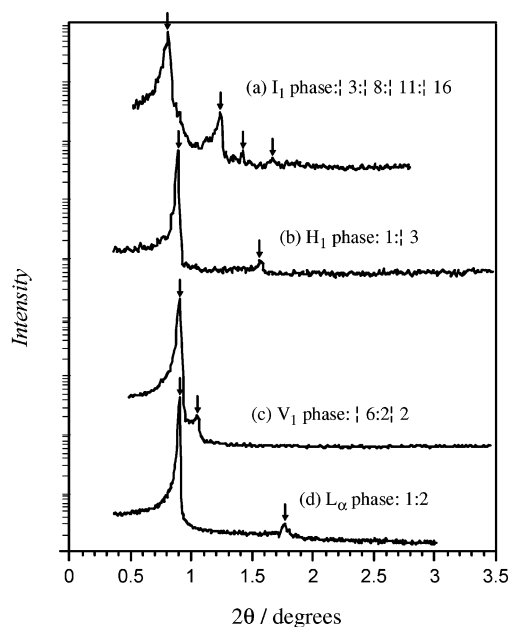
B. Determination of Phase Diagrams. The samples were prepared by weighing the appropriate amounts of the components in glass ampules. The ampules were flame-sealed immediately, and the sample mixtures were homogenized using a vortex device. Viscous samples were homogenized further by repeated centrifugation in both directions through a narrow constriction to facilitate mixing and then in one direction to speed up phase separation (if not single phase). The ampules were then equilibrated in a temperature-controlled bath at 25 °C for several days or weeks. Phases were identified by direct visual inspection and by observing the samples through cross polarizers. Small-angle X-ray scattering (SAXS) measurements were performed for a more quantitative identification of the different phases in both the binary and the ternary systems.

C. Small-Angle X-ray Scattering (SAXS). SAXS measurements were performed on a small-angle scattering goniometer equipped with an 18 kW rotating anode (RINT-2500, Rigaku, Tokyo). Ni-filtered Cu K α radiation ($\lambda = 1.541 \text{ \AA}$) was used. The applied voltage and filament current were 50 kV and 300 mA, respectively. Liquid crystal samples were covered by plastic films for the measurement (Mylar seal method). The interlayer spacing, d , of the liquid crystals was obtained from the first scattering peak. The microstructure of each liquid crystalline phase has been reported in a previous paper.⁸

III. Results and Discussion

A. Phase Behavior of the Binary Water/P85 System. The phase diagram of the binary P85/water system as a function of the temperature was determined, and it is shown in Figure 1.

The self-assembly of copolymer molecules depends on both copolymer concentration and temperature. In the water-rich part of the phase diagram, a micellar phase

**Figure 2.** SAXS spectra for liquid crystals at 25 °C in Figure 1: (a) I_1 phase at 39 wt %, (b) H_1 phase at 52.5 wt %, (c) V_1 phase at 68 wt %, and (d) L_α phase at 73 wt %.

region (W_m) extends up to $W_s = 0.315$ at 25 °C. In the concentrated region, micellar cubic (I_1 , 31.5–47.5 wt %), hexagonal (H_1 , 50–66.5 wt %), bicontinuous cubic (V_1 , 68–69.5 wt %), lamellar (L_α , 74–83 wt %), and solid copolymer phases (S) were successively formed with increasing W_s at 25 °C. The P85 layer curvature decreases with water content due to the dehydration of the polyoxyethylene chain. The maximum melting temperatures are around 56 °C for the I_1 phase, 82 °C for the H_1 phase, and 106 °C for the L_α phase. The minimum concentration required for the formation of the I_1 phase decreases as temperature increases because the formation of aggregates is favored by a decrease in the solubility of the PPO moiety.¹³

At high P85 concentrations, a reverse micellar solution phase (O_m) is found above the solid phase. The melting temperature of the solid decreases rapidly with increasing water content due to the hydration of the EO chains. The phase behavior of P85 is essentially the same as that of P105, except that the maximum temperature of liquid crystals is slightly lower.^{8,14}

B. Microstructure of P85 Liquid Crystals. To analyze the detailed structures of each liquid crystal in the P85 system, we measured the interlayer spacings of I_1 , H_1 , V_1 , and L_α phases as a function of copolymer concentration in the binary water–copolymer system by means of SAXS. The typical SAXS peaks are shown in Figure 2. The reciprocal spacings of these peaks are found to be in the ratio $\sqrt{3}:\sqrt{8}:\sqrt{11}:\sqrt{16}$ for the I_1 phase, $1:\sqrt{3}$ for the H_1 phase, $\sqrt{6}:2:\sqrt{2}$ for the V_1 phase, and 1:2 for the L_α phase. We interpret that the four peaks in the I_1 phase represent diffractions from the (111), (220), (311), and (400) planes, respectively. The indices of the planes indicate that this cubic phase has probably a face-centered-cubic (fcc) structure belonging to the $Fd3m$ space group,¹⁵ which is one of the typical space groups found for the discontinuous micellar cubic phases.

The characteristic parameters for the discontinuous cubic, hexagonal, and lamellar liquid crystalline phases were calculated assuming a spherical, rod, and bilayer aggregates in each liquid crystal.⁸ Their values are

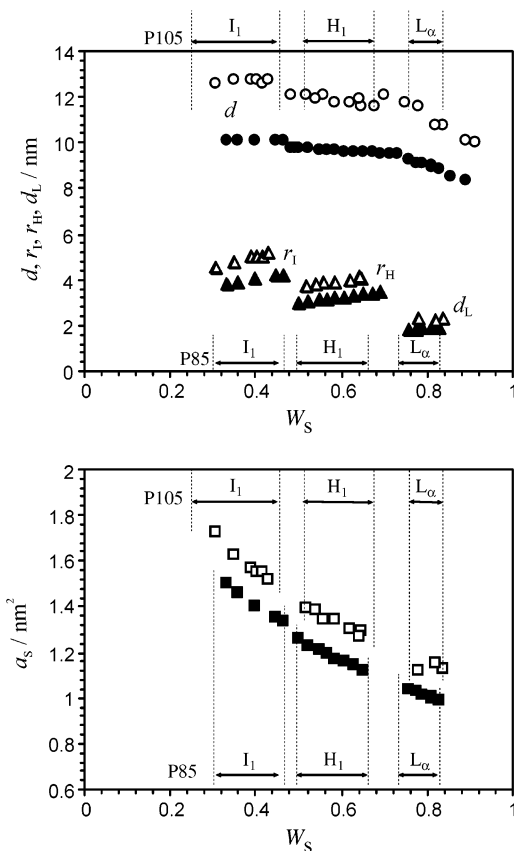


Figure 3. Change in structural parameters of liquid crystals as a function of W_S at 25 °C in the water/P85 system (filled symbols) and the water/P105 system⁸ (open symbols). Circles represent the interlayer spacing d , squares the effective cross-sectional area per headgroup a_s , and triangles the radius of spherical micelles in the I_1 phase, r_I , apolar cylinder radius in the H_1 phase, r_H , and half of the apolar film thickness in the L_α phase, d_L .

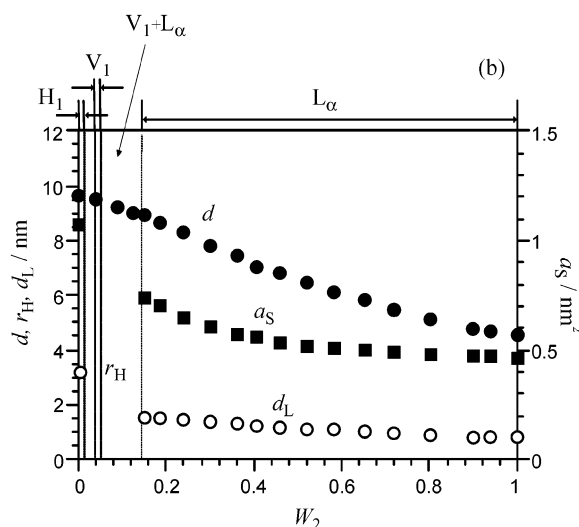


Figure 4. Change in structural parameters of liquid crystals in the water/P85/C₁₂EO₅ system as a function of the weight fractions of C₁₂EO₅ in total amphiphiles, W_2 , at 25 °C. The weight fraction of amphiphile in the system is fixed at 0.66.

shown together with those corresponding to the P105 system⁸ in Figure 3.

The interlayer spacing, d , gradually decreases with the water content. The effective cross-sectional area at the hydrophobic surface per molecule, a_s , also mono-

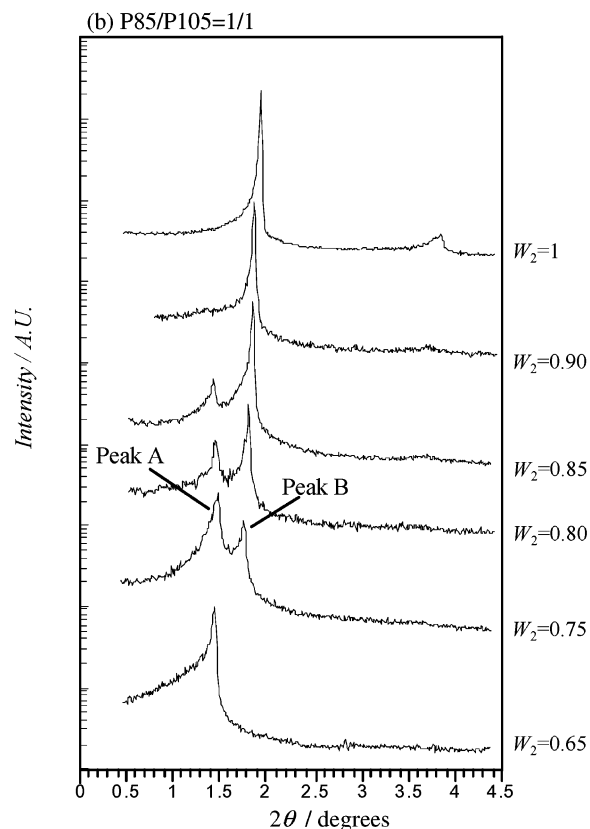
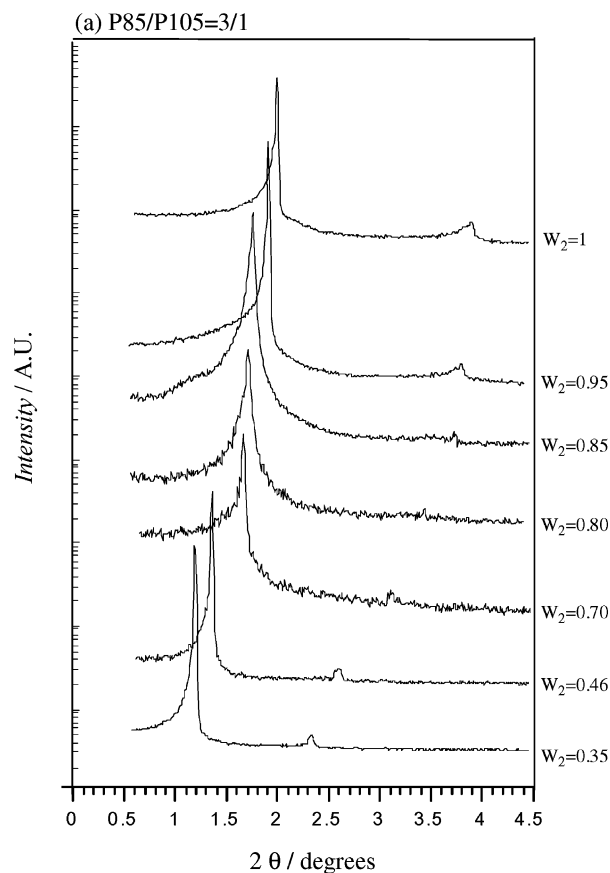


Figure 5. SAXS spectra in the water/P85/P105/C₁₂EO₅ system at 25 °C at different W_2 . W_S is fixed at 0.66. (a) P85/P105 = 3/1; (b) P85/P105 = 1/1.

tonically decreases. Hence, both the hydration of PEO chain and the repulsion between the hydrophilic moieties decrease with the water content. On the other

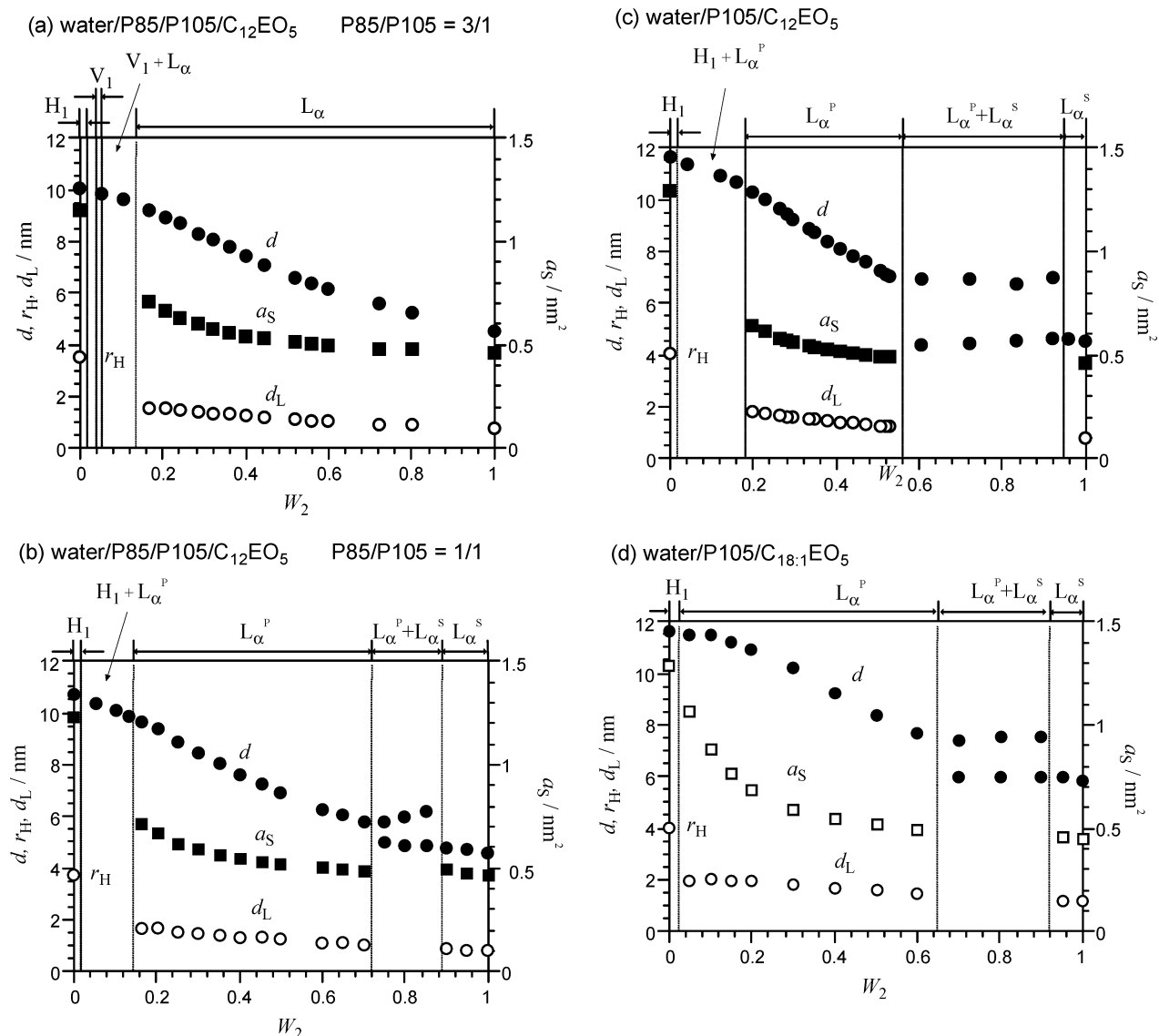


Figure 6. Change in structural parameters of liquid crystals in the water/copolymer/surfactant systems as a function of W_2 : (a) water/P85/P105/C₁₂EO₅, P85/P105 = 3/1; (b) water/P85/P105/C₁₂EO₅, P85/P105 = 1/1; (c) water/P105/C₁₂EO₅ (adapted from ref 8); (d) water/P105/C_{18:1}EO₅.

hand, the radius of spherical micelles, r_1 , increases with decreasing the water content. Actually, r_1 at the boundary between I_1 and H_1 phases is almost equal to the length of PPO chain in its extended state. This state is energetically unfavorable so that the hydrophobic chains tend to shrink, and r_1 , r_H , and d_L decrease when the phase transitions I_1 – H_1 – L_α takes place with a simultaneous decrease in a_S . In the P105 system, d and the other structural parameters have the same tendency as that in the P85 system.

C. Phase Transition by Substituting P85 with C₁₂EO₅. We measured the SAXS spectra in P85–C₁₂EO₅ at a constant amphiphile concentration ($W_S = 0.66$) by replacing P85 with C₁₂EO₅. The interlayer spacing continuously decreases, and the hexagonal phase in the water/P85 system changes to a lamellar phase up to 100% C₁₂EO₅, as shown in Figure 4. Within the L_α phase, the interlayer spacing shows no discontinuity, indicating that phase separation does not take place. In our previous report,⁸ the hexagonal phase in the water/P105 system also changes to a lamellar phase by substitution of the copolymer with C₁₂EO₅. However,

two lamellar phases coexist in the water/P105/C₁₂EO₅ system: one is polymer-rich and another is surfactant-rich.

The interlayer spacing is ~ 9 nm for the P85-rich L_α phase at the boundary with the two-phase region ($V_1 + L_\alpha$), and the area per PEO block at the hydrophobic interface is ~ 0.75 nm². The lamellar phase in the C₁₂EO₅-rich region exhibits a smaller interlayer spacing (~ 4.5 nm) and interfacial area (~ 0.45 nm²) at 100% C₁₂EO₅. Since C₁₂EO₅ is dissolved in the palisade layer of P85 lamellar phase, the average a_S and d_L decreases with increasing the C₁₂EO₅ content in the lamellar phase. Although d_L in the mixed system is much smaller than that in water/P85 system shown in Figure 3, there is still space to contain the long hydrophobic PPO chain in the bilayer, and no phase separation takes place.

D. Phase Behavior and Microstructure of Lamellar Phases in the Water/P85/P105/C₁₂EO₅ System. In our previous paper,⁸ it was found that two lamellar phases coexist in the water/P105/C₁₂EO₅ system, in which the P105 lamellar phase dissolves a considerable amount of C₁₂EO₅, whereas P105 is practically insoluble

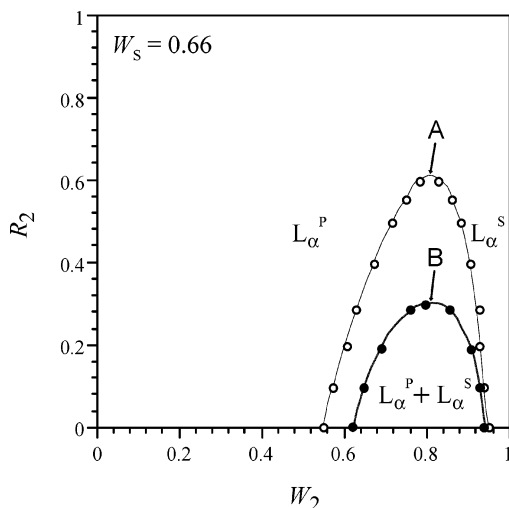


Figure 7. Miscibility gap between coexisting lamellar phases ($L_{\alpha}^P + L_{\alpha}^S$) in the water/P85/P105/C₁₂EO₅ system (open symbols) and the water/P85/P105/C_{18:1}EO₅ system (filled symbols) at $W_S = 0.66$. W_2 is the weight fraction of C₁₂EO₅ in total amphiphile. R_2 is the weight fraction of P85 in copolymer mixture. L_{α}^S and L_{α}^P denote the surfactant-rich lamellar and copolymer-rich lamellar phase, respectively. The H₁ phase region is omitted in the figure.

in the C₁₂EO₅ lamellar phase. Since the PPO chain of P105 is too large to be incorporated in the C₁₂EO₅ bilayer, phase separation occurs. Hence, it is considered that phase separation would be inhibited by replacing P105 with P85.

SAXS spectra of lamellar phases in the water/P85/P105/C₁₂EO₅ system at $W_2 = 0.35$ – 1.0 are shown in Figure 5. At a copolymer mixing ratio P85/P105 = 3/1, first and second Bragg peaks are observed, indicating formation of one type of lamellar phase. However, at P85/P105 = 1/1, a third peak, located at $2\theta = 1.5^\circ$ (peak A), is observed for $W_2 = 0.75$, where W_2 is the weight fraction of surfactant in surfactant + copolymers. The intensity of peak A decreases whereas the intensity of the second peak (peak B) increases with increasing W_2 . In the two-lamellar-phase region, the position of peaks A and B remains constant, which means that the composition change in Figure 5b occurs almost along the tie line joining copolymer-rich and surfactant-rich lamellar phases.

The measured d and calculated d_L and a_S for lamellar phase in the water/P85/P105/C₁₂EO₅ system at $W_S = 0.66$ are shown in Figure 6, where the P85/P105 weight ratio is 3/1 for Figure 6a and 1/1 for Figure 6b. With increasing W_2 (C₁₂EO₅ content), the interlayer spacing largely decreases because small C₁₂EO₅ is dissolved in the copolymer layer. a_S also shows a large decrease, and phase separation takes place at P85/P105 = 1/1.

The structural parameters for liquid crystals in water/P105/C₁₂EO₅ systems and water/P105/C_{18:1}EO₅ systems are shown in Figure 6c,d. In both systems, d , d_L , and a_S monotonically decrease; however, the decrease in the bilayer thickness is smaller for C_{18:1}EO₅ systems than for C₁₂EO₅ systems. Hence, the copolymer hydrophobic chain can be more easily incorporated at a certain mixing fraction, and the two lamellar-phase region shrinks in the system with C_{18:1}EO₅.

The mutual solubility between lamellar phases is shown in Figure 7. When the average molecular weight of the copolymer mixture decreases, the miscibility gap shrinks. The same effect is produced by increasing the

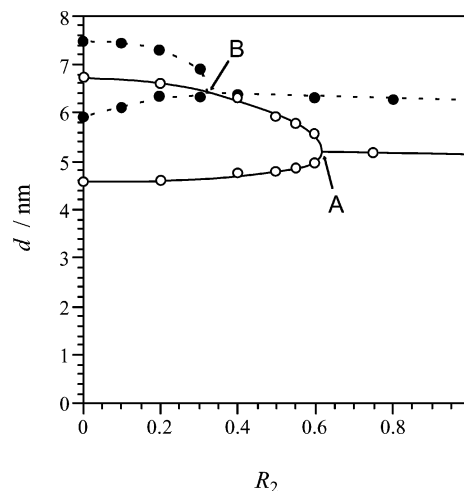


Figure 8. Interlayer spacing obtained from SAXS spectra measured at $W_2 = 0.8$ in Figure 7. Open symbols are for the water/P85/P105/C₁₂EO₅ system, and filled symbols are for the water/P85/P105/C_{18:1}EO₅ system.

surfactant molecular weight. The change in interlayer spacing was measured at $W_2 = 0.8$ in Figure 7 and is shown in Figure 8. Both d values are coincident at the top of two-lamellar-phase region (points A and B), and only one lamellar phase is formed at a higher P85 content. Hence, it is considered that point A or B is an isothermal critical solution point (plait point) for two lamellar phases. The degree of freedom for a critical point is expressed by the following equation¹⁶

$$f - c - p + 2 - (p' - 1) \quad (1)$$

where c is the number of components, p is the number of phases, and p' is the number of phases that become identical at the critical point. In the present system, roughly $c = 4$, $p = p' = 2$, and $f = 3$ if each copolymer is regarded as one component. Since temperature, pressure, and the concentration of water are fixed, $f = 0$ at points A and B in Figures 7 and 8.

E. Change in Microstructure of Lamellar Phases as a Function of Amphiphilic Composition. The change in the a_S in Figure 6 was plotted against the mole fraction of surfactant in surfactant + copolymer, X_2 , and is shown in Figure 9. a_S continuously decreases with increasing X_2 . Since the surfactant molecular weight is very low compared with that of copolymer, the phase separation takes place at a very high X_2 . Hence, the bilayer of lamellar phase consists mainly of surfactant molecules, even in the polymer-rich lamellar phase near the phase separation boundary. The data in Figure 9 show a nonlinear tendency, indicating nonideal mixing of surfactant and copolymer molecules at the interface in the bilayer.

Analogous to the partial molar volume for nonideal mixing of two liquids,¹⁷ here we define the partial molecular areas as follows:

$$a_S^P = f(X_2) - \frac{df(X_2)}{dX_2} X_2 \quad (2)$$

$$a_S^S = f(X_2) + \frac{df(X_2)}{dX_2} (1 - X_2) \quad (3)$$

where $f(X_2)$ is the function derived from fitting a_S data to a polynomial (quadratic). The values for a_S^P and a_S^S

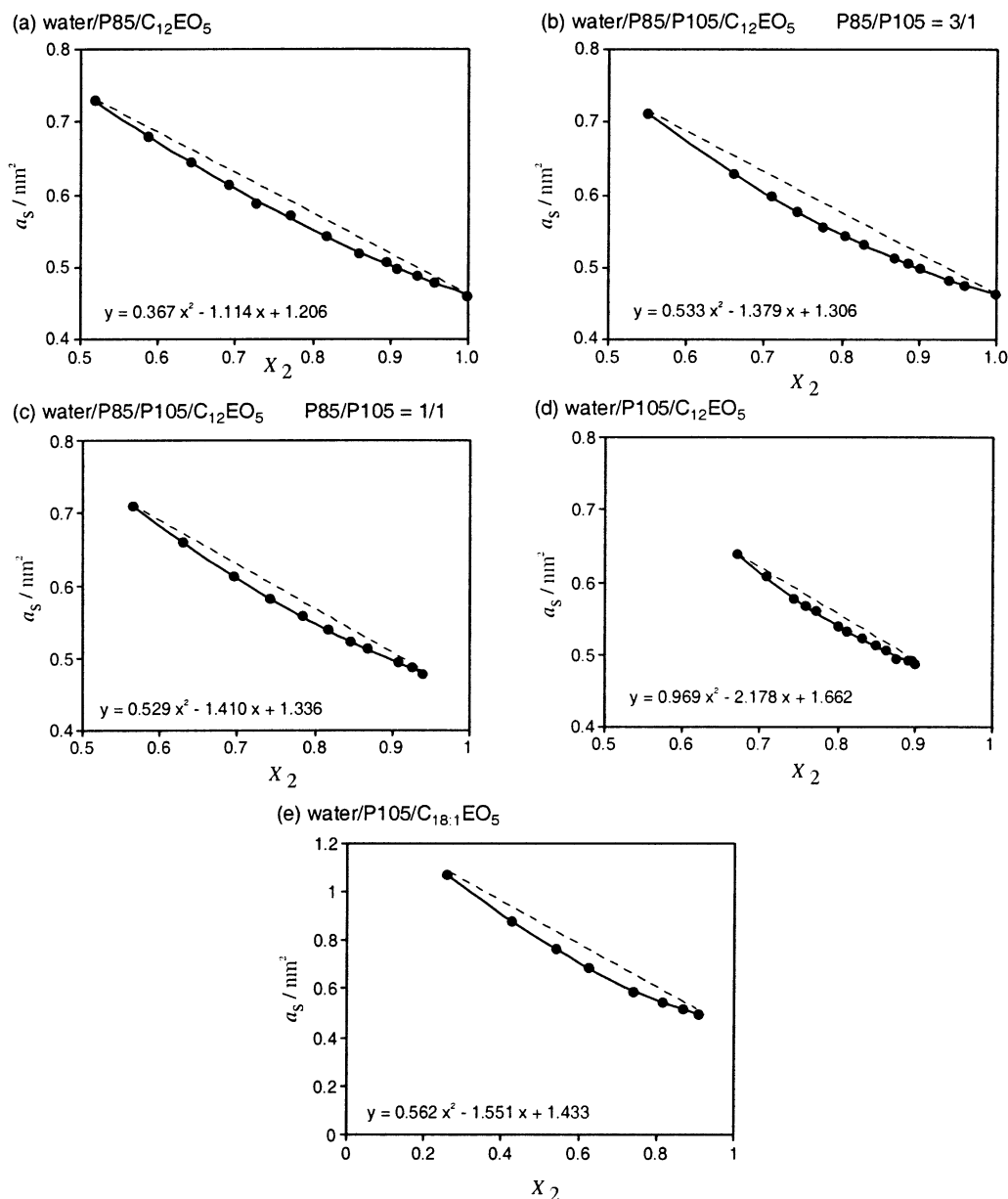


Figure 9. Effective cross-sectional area per hydrophilic group of amphiphilic molecule, a_S , in Figure 6 plotted against mole fraction of surfactant in total amphiphiles, X_2 , for the (a) water/P85/C₁₂EO₅ system, (b) water/P85/P105/C₁₂EO₅ system at P85/P105 = 3/1, (c) water/P85/P105/C₁₂EO₅ system at P85/P105 = 1/1, (d) water/P105/C₁₂EO₅ system, and (e) water/P105/C_{18:1}EO₅ system. Dashed lines indicate ideal mixing. The continuous lines and the equations in the figures represent the best fit to a_S values.

are shown in Figure 10. In the water/P85/P105/C₁₂EO₅ system, a_S^P decreases and a_S^S increases with increasing X_2 at every P85/P105 ratio. The hydrophobic bilayer thickness which corresponds to $2d_L$ decreases with increasing X_2 , as is shown in Figure 6. Molecular packing of amphiphile at the interface is determined as the result of the balance between attractive force originating from reducing interfacial energy (interfacial tension) and repulsive force originating from steric hindrance or hydration force.¹⁸ When surfactant molecules that have a much shorter poly(oxyethylene) chain than the copolymer are added among copolymer molecules in the copolymer-rich bilayer, the distance between neighboring poly(oxyethylene) chains of copolymer increases. This induces the reduction of the repulsive force between the copolymer poly(oxyethylene) chains and also the reduction of occupied area of a copolymer chain to keep the balance with the interfacial tension.¹⁹

Hence, the molecular area of copolymer, a_S^P , decreases with increasing X_2 , as is shown in Figure 11. On the other hand, the repulsive force between neighboring surfactant poly(oxyethylene) chains increases with increasing X_2 since the number of surfactant molecules that have smaller molecular area than copolymer increases. Hence, the a_S^S increases with X_2 .

In the hydrophobic bilayer, when the surfactant molecules are added in the copolymer-rich lamellar phase, the poly(oxypropylene) chains of copolymer have to shrink and expand laterally since d_L of the L_α^P phase is longer than the length of surfactant hydrophobic chain in the lamellar phase, which corresponds to the d_L of the water/C₁₂EO₅ system, as is shown in Figure 6. Therefore, the hydrophilic layer thickness decreases as increasing X_2 , as is shown in Figure 11.

The values of a_S^P and a_S^S in the water/P105/C_{18:1}EO₅ system are presented in Figure 10e. It is again observed

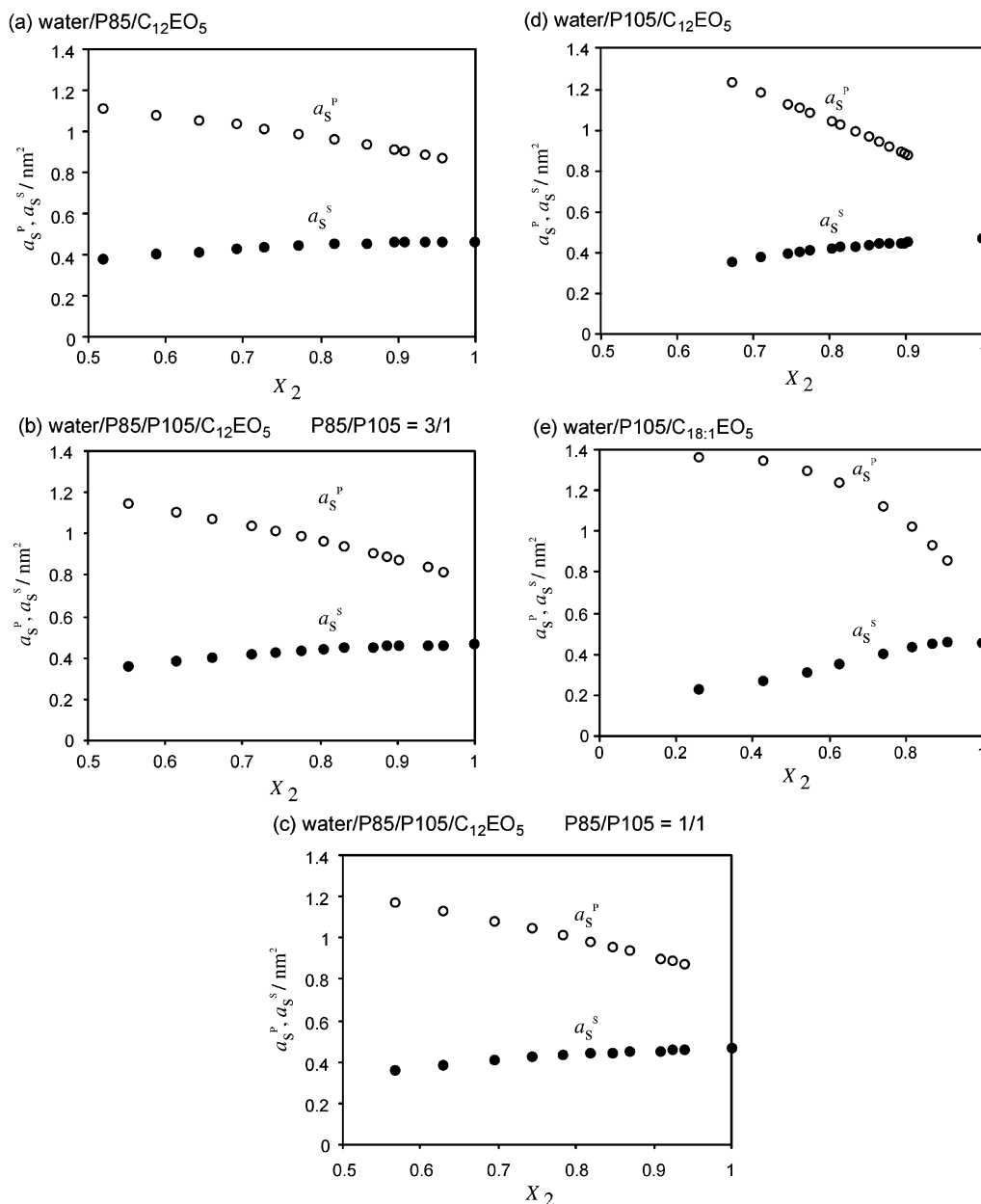


Figure 10. Partial molar area of copolymer, a_S^P , and surfactant molecule, a_S^S , for the (a) water/P85/C₁₂EO₅ system, (b) water/P85/P105/C₁₂EO₅ system at P85/P105 = 3/1, (c) water/P85/C₁₂EO₅ system at P85/P105 = 1/1, (d) water/P105/C₁₂EO₅ system, and (e) water/P105/C_{18:1}EO₅ system.

that a_S^P decreases and a_S^S increases as the system approaches the phase separation boundary. However, at low surfactant fractions, a_S^S is smaller for C_{18:1}EO₅ than for C₁₂EO₅, and as a consequence, a_S^P is larger. This fact contributes to a decrease of the lateral pressure in the bilayer, which facilitates the incorporation of additional molecules in the L _{α} phase.

IV. Concluding Remarks

In a water–copolymer system, the phase behavior of P85 is very similar to that of P105, and the phase sequence is the same: aqueous micellar solution, micellar cubic, hexagonal, bicontinuous cubic, and lamellar phases are formed with increasing copolymer concentration.

P85 forms a single lamellar phase with C₁₂EO₅ in a wide range of mixing fraction at constant water content. On the other hand, higher molecular weight P105 forms

a lamellar phase with a large amount of C₁₂EO₅, which coexists with another lamellar phase consisting of almost pure C₁₂EO₅.

By mixing P85 with P105, the two-lamellar-phase region is reduced and eventually disappears at a critical point, at which two lamellar phases become identical. When C₁₂EO₅ is substituted with a longer hydrophobic chain surfactant (C_{18:1}EO₅), the two-lamellar-phase region is reduced because the bilayer is more capable to contain the long hydrophobic chains of copolymer.

The partial molecular area of copolymer and surfactant at the interface, a_S^S and a_S^P , can be evaluated from average molecular area of mixed amphiphiles at various mixing fractions. In all the systems presented here, a_S^S decreases and a_S^P increases with the increase in surfactant content in the mixed amphiphiles. Bilayer thickness is reduced with decreasing surfactant content in all the systems. These suggest that the repulsion

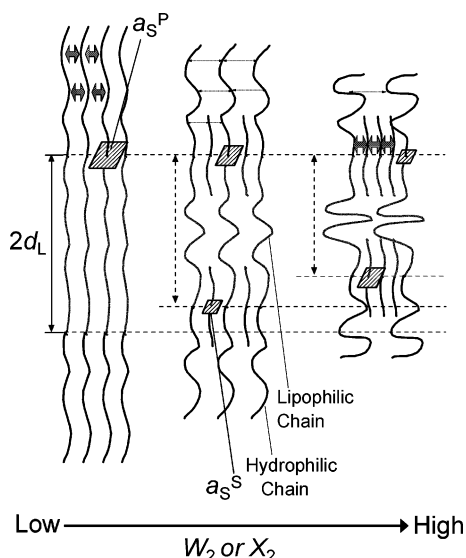


Figure 11. Schematic illustration of the change in bilayer structure at different surfactant concentrations in copolymer-surfactant mixtures.

between neighboring copolymer (surfactant) poly(oxyethylene) chains decreases and poly(oxypropylene) chains in hydrophobic bilayer shrink and expand laterally.

Acknowledgment. C.R. is grateful to the Japanese Society for the Promotion of Science (JSPS) for a research grant during his stay at Yokohama National University.

References and Notes

- (1) Alexandridis, P. *Curr. Opin. Colloid Interface Sci.* **1997**, *2*, 478.
- (2) Glatter, O.; Scherf, G.; Schiller, K.; Brown, W. *Macromolecules* **1994**, *27*, 6046.
- (3) Wanka, G.; Hoffmann, H.; Ulbricht, W. *Macromolecules* **1994**, *27*, 4.
- (4) Hamley, I. W.; Mortensen, K.; Yu, G. E.; Booth, C. *Macromolecules* **1998**, *31*, 6958.
- (5) Alexandridis, P. *Curr. Opin. Colloid Interface Sci.* **1996**, *1*, 490.
- (6) Kunieda, H.; Uddin, Md. H.; Furukawa, H.; Harashima, A. *Macromolecules* **2001**, *34*, 9093.
- (7) Singer, S. J.; Nicolson, G. L. *Science* **1972**, *175*, 720.
- (8) Hossain, M. K.; Hinata, S.; Lopez-Quintela, A.; Kunieda, H. *J. Dispersion Sci. Technol.* **2003**, *24*, 411.
- (9) Fontell, K.; Ceglie, A.; Lindman, B.; Ninham, B. *Acta Chem. Scand.* **1986**, *40*, 247-256.
- (10) Kunieda, H.; Shigeta, K.; Ozawa, K.; Suzuki, M. *J. Phys. Chem. B* **1997**, *101*, 7952.
- (11) Huang, K.-L.; Shigeta, K.; Kunieda, H. *Prog. Colloid Polym. Sci.* **1998**, *110*, 171.
- (12) Brown, W.; Schillen, K.; Almgren, M.; Hvidt, S.; Bahadur, P. *J. Phys. Chem.* **1991**, *95*, 1850.
- (13) Bryskhe, K.; Schillen, K.; Lofroth, J.-E.; Olsson, U. *Phys. Chem. Chem. Phys.* **2001**, *3*, 1304.
- (14) Alexandridis, P.; Zhou, D.; Khan, A. *Langmuir* **1996**, *12*, 2690.
- (15) Hahn, T., Ed. *International Tables for Crystallography*; Reidel: Dordrecht, Holland, 1983; Vol. A.
- (16) Zernike, J. *Pays-Bas* **1949**, *68*, 585.
- (17) Atkins, P. W. *Physical Chemistry*, 5th ed.; Oxford University Press: Oxford, 1994; p 208.
- (18) Istaclachvili, J. N. *Intermolecular and Surface Forces*, 2nd ed.; Academic Press: London, 1992; p 367.
- (19) Kunieda, H.; Umizu, G.; Aramaki, K. *J. Phys. Chem. B* **2000**, *104*, 2005.

MA0350664